SMAR 2019

Damage experiment on a steel plate girder bridge and local damage detection utilizing traffic-induced vibration

Chul-Woo KIM [1], Yoshinao GOI [1], Takuya MIMASU [1]
[1] Kyoto University, Kyoto, Japan

Contact e-mail: kim.chulwoo.5u@kyoto-u.ac.jp

ABSTRACT: This study is intended to investigate feasibility of local damage detection on a steel plate girder bridge utilizing traffic-induced vibration. A field experiment on the bridge was conducted, and acceleration responses of the bridge under a single moving vehicle were monitored. Fatigue cracks observed in actual steel plate girder bridges were considered in the experiment, and artificial damages were introduced to the girder. Firstly, changes in the modal frequencies of the steel plate girder bridge due the artificial damages are investigated. The modal properties identified from the experiment are comparable to the relevant finite element model. Secondly, a damage sensitive feature from system matrces is introduced, and feasibility of detecting local damage by means of Bayesian hypothesis testing is examined. The damage sensitive features correspond to the modal properties identified in the experiment. The proposed hypothesis test successfully detected anomaly event due to the local damage. Furthermore, the location of the damage is roughly estimated by the proposed damaged indicator.

1 INTRODUCTION

Management of aging infrastructure is a crucially important issue confronting civil engineering professionals. To reduce the potential risk of structural failure as well as life cycle costs, an efficient inspection method is desirable for preventive maintenance. Techniques of structural health monitoring (SHM) based on vibration measurements have been attracting bridge authorities. Changes in structural integrity of bridges engender changes in their modal properties that are identifiable from vibration data (Deramaeker et al. 2007, Zhang, 2007). For an actual truss bridge, Chang & Kim (2016) verified feasibility for damage detection using its modal properties.

To detect changes in the modal properties effectively, several studies have developed damage indicators that are directly defined from a mechanical system model representing the bridge vibration. For instance, Nair et al. (2006) investigated damage sensitive-feature consisting of univariate autoregressive (AR) coefficients for a model building. To enable reliable decision-making for bridge maintenance, the authors newly proposed the damage indicator using Bayesian statistics and verified feasibility for damage detection on the actual truss bridge (Goi & Kim, 2017). The proposed damage indicator is referred as Bayes factor in this study.

This study investigates the feasibility of the vibration-based SHM to detect fatigue cracks on steel plate girder bridges. A damage experiment on an actual plate girder bridge is performed introducing artificial cracks on the girder. The modal frequencies of the target bridge and the proposed Bayes factor are respectively assessed to detect the introduced damage. Also, a finite element (FE) model of the target bridge is composed to investigate the mechanical behavior of the bridge before and after the damage.

2 METHODOLOGY

2.1 Modal identification

This study adopts the stochastic subspace identification (SSI) (van Overschee & De Moor, 1996) to identify the modal properties of the target bridge from the experimental data. The dynamic system is modeled as the following state space model

$$\begin{aligned}\mathbf{x}(k+1) &= \mathbf{A}\mathbf{x}(k) + \mathbf{w}(k)\\ \mathbf{y}(k) &= \mathbf{C}\mathbf{x}(k) + \mathbf{v}(k)\end{aligned} \tag{1}$$

where $\mathbf{x}(k)$ and $\mathbf{y}(k)$ respectively represent the state vector of structure and vector of the measured data at each time step k. $\mathbf{w}(k)$ and $\mathbf{v}(k)$ respectively denote the process noise and measurement noise. They are assumed as stationary white noise. System matrices **A** and **C** are estimated by means of the least square method for minimal prediction error of the state $\mathbf{x}(k)$ given by the forward Kalman filter. The poles of the dynamic system provide modal properties of the dynamic system.

The algorithm for the SSI is described as follows briefly. Firstly, we obtain the projection matrix $\boldsymbol{O}_i$ that is estimated as follows.

$$\boldsymbol{O}_i = \mathbf{Y}_\mathrm{f}\mathbf{Y}_\mathrm{p}^\mathrm{T}\left(\mathbf{Y}_\mathrm{p}\mathbf{Y}_\mathrm{p}^\mathrm{T}\right)^\dagger\mathbf{Y}_\mathrm{p} \tag{2}$$

where $(\;\cdot\;)^\dagger$ denotes the Moore-Penrose pseudo inverse matrix. $\mathbf{Y}_f$ and $\mathbf{Y}_p$ are the block Hankel matrices defined as follows.

$$\begin{pmatrix}\mathbf{Y}_\mathrm{p}\\ --\\ \mathbf{Y}_\mathrm{f}\end{pmatrix} = \left[\begin{array}{ccc}\mathbf{y}(0) & \dots & \mathbf{y}(j-1)\\ \vdots & \ddots & \vdots\\ \mathbf{y}(i-1) & \dots & \mathbf{y}(i+j-2)\\ \hline \mathbf{y}(i) & \dots & \mathbf{y}(i+j-1)\\ \vdots & \ddots & \vdots\\ \mathbf{y}(2i-1) & \dots & \mathbf{y}(2i+j-2)\end{array}\right] \tag{3}$$

The singular value decomposition (SVD) is then applied to factorize $\boldsymbol{O}_i$ as

$$\boldsymbol{O}_i = \mathbf{U}\mathbf{S}\mathbf{V}^\mathrm{T} = (\mathbf{U}_1\mathbf{U}_2)\begin{pmatrix}\mathbf{S}_1 & 0\\ 0 & \mathbf{S}_2\end{pmatrix}(\mathbf{V}_1\mathbf{V}_2)^\mathrm{T} \simeq \mathbf{U}_1\mathbf{S}_1\mathbf{V}_1^\mathrm{T} \tag{4}$$

where **U** and **V** are unitary matrices with an appropriate size, and **S** is a matrix whose diagonal elements are non-negative and the other elements are 0. The diagonal elements of **S** are known as singular values of $\boldsymbol{O}_i$. Letting singular values in **S** be listed in descending order, the components in $\mathbf{U}_1\mathbf{S}_1\mathbf{V}_1^\mathrm{T}$ mostly approximate the elements in $\boldsymbol{O}_i$. The state sequence $\mathbf{X}_i = [\mathbf{x}(i) \quad \mathbf{x}(i+1) \quad \dots \quad \mathbf{x}(i+j-1)]$ predicted by the Kalman filter in least square sense is obtained as follows.

$$\mathbf{X}_i = \mathbf{S}_1^{1/2}\mathbf{V}_1^\mathrm{T} \tag{5}$$

The system matrices **A** and **C** in Eq. 1 are estimated using the state sequence given as Eq. 5. The modal properties are converted from the estimated system matrices according to the well-known modal analysis theory (Heylen et al., 1997).

2.2 Damage indicator

This study adopts Bayes factor which is previously proposed by the authors (Goi & Kim, 2017). Let the reference data is given from a healthy bridge, and test data is newly observed from the bridge whose health condition is unknown. The proposed Bayes factor assess whether the dynamic properties of the test data is changed from the ones of reference data or not.

The linear system model given in Eq. 1 can be simplified to the following vector autoregressive model (He & De Roeck, 1999).

$$\mathbf{y}(k) = \mathbf{W}\begin{bmatrix}\mathbf{y}(k-1)\\ \vdots \\ \mathbf{y}(k-p)\end{bmatrix} + \mathbf{v}(k) \qquad (6)$$

where $\mathbf{W}$ stands for the matrix composed of the regressive coefficients for the vector autoregressive model. It is known that the modal properties can be estimated from those regressive coefficients (Heylen et al., 1997). The proposed method assumes Gaussian noise for the noise vector $\mathbf{v}(k)$, and provides hypothesis testing to detect changes in the modal properties by evaluating the changes in the regressive coefficients. To localize damage, this study adopts the following regressive model which corresponds to the *j*-th raw of the Eq. 6.

$$y^{\{j\}}(k) = \boldsymbol{w}^{\{j\}}\begin{bmatrix}\mathbf{y}(k-1)\\ \vdots \\ \mathbf{y}(k-p)\end{bmatrix} + v^{\{j\}}(k) \qquad (7)$$

where $y^{\{j\}}(k)$ and $v^{\{j\}}(k)$ respectively stand for the *j*-th element of the vectors $\mathbf{y}(k)$ and $\mathbf{v}(k)$, and $\boldsymbol{w}^{\{j\}}$ stands for the *j*-th raw of the matrix W.

Bayesian inference (Bishop, 2016) enables to produce posterior distribution of the regressive coefficient according to the following Bayes theorem.

$$\mathrm{p}\left(\boldsymbol{w}^{\{j\}}, \sigma_j^2 \middle| \mathcal{D}_\mathrm{r}^{\{j\}}\right) = \frac{\mathrm{p}\left(\mathcal{D}_\mathrm{r}|\boldsymbol{w}^{\{j\}},\sigma_j^2\right)\mathrm{p}\left(\boldsymbol{w}^{\{j\}},\sigma_j^2\right)}{\mathrm{p}(\mathcal{D}_\mathrm{r})} \qquad (8)$$

where $\mathrm{p}(\cdot)$ denotes the probability density function (PDF), σ_j^2 denotes the variance of the *j*-th element of the noise vector $v^{\{j\}}(k)$, $\mathcal{D}_\mathrm{r}^{\{j\}}$ represents the reference data obtained from the *j*-th measurement location on the bridge under healthy condition, and $\mathrm{p}\left(\mathcal{D}_\mathrm{r}^{\{j\}}|\boldsymbol{w}^{\{j\}}, \sigma_j^2\right)$ stands for the likelihood function for the matrices $\boldsymbol{w}^{\{j\}}$ and σ_j^2. Assuming non-informative prior (Jeffreys, 1946), the posterior distribution is converted from the likelihood function, which is easily given from the regressive model in Eq. 7.

According to the functional form of the posterior distribution, the parameters with low variance are extracted from the regressive coefficients. This study regards those extracted parameters as damage-sensitive features. The hypothesis testing to detect changes in the damage sensitive features of the test data is formulated through the PDFs representing the following two hypotheses $\mathrm{p}\left(\boldsymbol{w}^{\{j\}}, \sigma_j^2 \middle| \mathcal{H}_0\right)$ and $\mathrm{p}\left(\boldsymbol{w}^{\{j\}}, \sigma_j^2 \middle| \mathcal{H}_1\right)$, where $\mathrm{p}\left(\boldsymbol{w}^{\{j\}}, \sigma_j^2 \middle| \mathcal{H}_0\right)$ denotes the null hypothesis for which the damage sensitive features are not altered from the reference data and $\mathrm{p}\left(\boldsymbol{w}^{\{j\}}, \sigma_j^2 \middle| \mathcal{H}_1\right)$ denotes the alternative hypothesis for which the damage sensitive features are altered from the reference data. The above two PDFs respectively provide evidence functions for the test data as

$$\mathrm{p}\left(\mathcal{D}_\mathrm{t}^{\{j\}}|\mathcal{H}_\kappa\right) = \iint \mathrm{p}\left(\mathcal{D}_\mathrm{t}^{\{j\}}|\boldsymbol{w}^{\{j\}}, \sigma_j^2\right)\mathrm{p}\left(\boldsymbol{w}^{\{j\}}, \sigma_j^2|\mathcal{H}_\kappa\right)\mathrm{d}\boldsymbol{w}^{\{j\}}\mathrm{d}\sigma_j^2 \ \ (\text{for } \kappa = 0{,}1) \qquad (9)$$

where $\mathcal{D}_\mathrm{t}^{\{j\}}$ represents the test data obtained from the *j*-th measurement location. The Bayes factor is defined as the ratio of the two evidence functions, i.e.,

$$B^{\{j\}} = \frac{\mathrm{p}\left(\mathcal{D}_\mathrm{t}^{\{j\}}|\mathcal{H}_1\right)}{\mathrm{p}\left(\mathcal{D}_\mathrm{t}^{\{j\}}|\mathcal{H}_0\right)} \qquad (10)$$

Kass and Raftery (1995) suggested interpreting the Bayes factor on the logarithm scale. For example, if $2\ln B$ is over 10, then the evidence of the alternative hypothesis $\mathcal{H}_1$ against the null hypothesis $\mathcal{H}_0$ is interpreted to be '*very strong*'. This study thus investigates the logarithm-scaled Bayes factor $2\ln B^{\{j\}}$ as a damage indicator.

3 FIELD EXPERIMENT AND NUMERICAL MODEL

3.1 Field experiment

The field experiment was conducted on an actual steel plate girder bridge as shown in Fig. 1 where sensor deployment is also appeared. The span length of the bridge is 40m and width of the bridge is 4.0m. Ten accelerometers were installed on the lower flanges to measure the vertical vibrations. The displacements of the both ends of the span were measured by displacement sensors. Artificial damages imitating fatigue cracks at the girder end near the base plate of the supports were introduced by severing the lower flange and the web plate with an Oxyacetylene cutting torch. The location of the artificial damage is at the east main girder on the bearing at Ab1 abutment (see Fig. 1). Fig. 2 shows the detailed damage location. The artificial damage comprises two damage levels. One is the lower flange cut (hereafter called DMG1) and another is the web plate cut (hereafter called DMG2). The bridge condition before the artificial damage is regarded as the intact condition (hereafter called INT).

3.2 Finite element model

To investigate the structural characteristics of the bridge, the eigenvalue analysis using the FE model of the bridge was conducted by utilizing ABAQUS 6.14. The bridge model, shown in

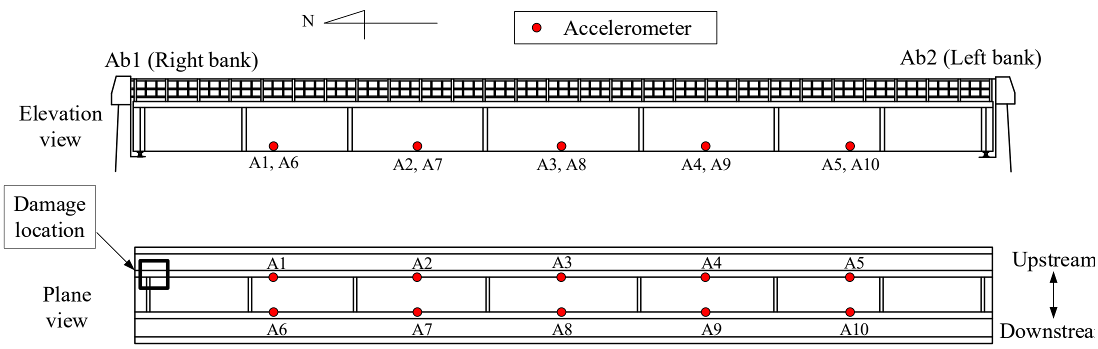

Figure 1. Sensor deployment and damage scenario.

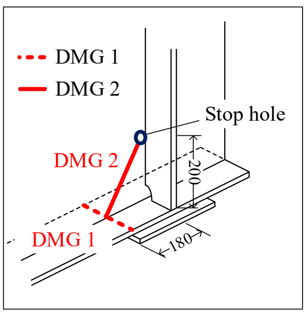

Figure 2. Detailed damage location.

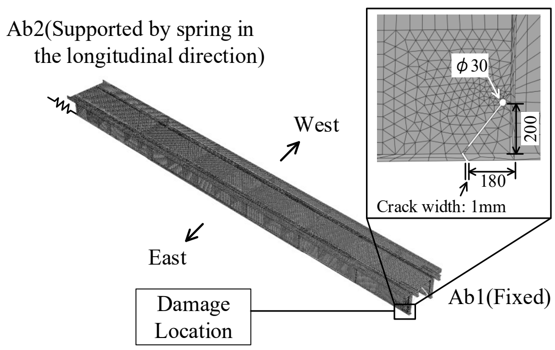

Figure 3. Finite element model.

Fig. 3, was built based on the documents of periodic inspection and information obtained from the field experiment for the original design documents of this bridge are not available. The concrete deck, main girder, vertical stiffener and horizontal stiffeners were modelled with shell element, and cross beam and lateral bracing were modelled with beam element. According to the results obtained from the static loading test, the boundary conditions were given as follows: Fixed supports were assumed on the Ab1 abutment, and roller supports with longitudinal springs were assumed on the Ab2 abutment. Specific gravities of steel and concrete were assumed as 7.85 and 2.40 respectively. Young's moduli of steel and reinforced concrete were assumed as 210 GPa and 22.02 GPa, respectively.

Since the bridge model has some differences from the actual bridge due to deterioration and construction errors, the bridge model needs model updating for calibration of structural parameters. The cross entropy (CE) method was applied to update the bridge model so that the natural frequencies of the bridge model become comparable to those of the actual bridge (McGetrick et al., 2015). The spring constant on Ab2 abutment was calibrated by the model update, and the artificial damages introduced in the field experiment were modelled as pseudo cracks in the updated FE model to investigate the change in structural characteristics. This crack was created by removing the connection of elements (see Fig. 3). The eigenvalue analysis was conducted for each damage scenario considered in the field experiments.

4 RESULTS

4.1 Identified modal properties

Mode shapes identified from the experimental vibration data by means of the SSI method are shown in Fig. 4. This study focuses on three bending modes and the two torsional modes which were stably identified.

Histograms of the identified frequencies in each bridge condition are shown in Fig. 5 with normal distribution fits, where the bin width was chosen as 0.01Hz. The histogram was created utilizing 30 samples of the identified frequencies. The statistical distributions show that frequencies for the 2nd and 3rd bending modes and the 2nd torsional mode tend to decrease as damage becomes severe, i.e., in the order of INT, DMG1 and DMG2. It demonstrates decrease of bending stiffness of the plate girder due to the artificial damage. However, the frequencies of the 1st bending mode and the 1st torsional mode tend to increase as damage becomes severe.

Frequencies and mode shapes from the eigenvalue analysis utilizing the calibrated FE model are compared to those identified from monitoring data. In the model calibration, using the experiment data of INT scenario as reference, the initial finite element model is correlated and tuned towards frequencies. The calibrated FE model of the bridge led to eigen-frequencies of 3.13Hz, 9.36Hz,

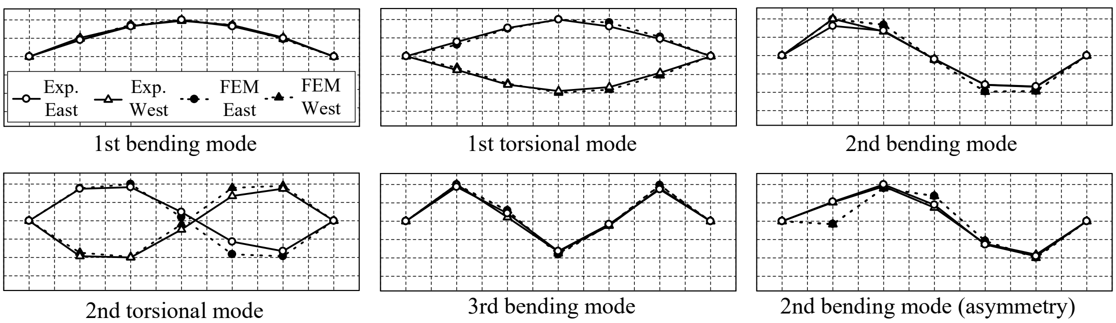

Figure 4. Mode shapes identfied from the FE model and the experimental vibration data.

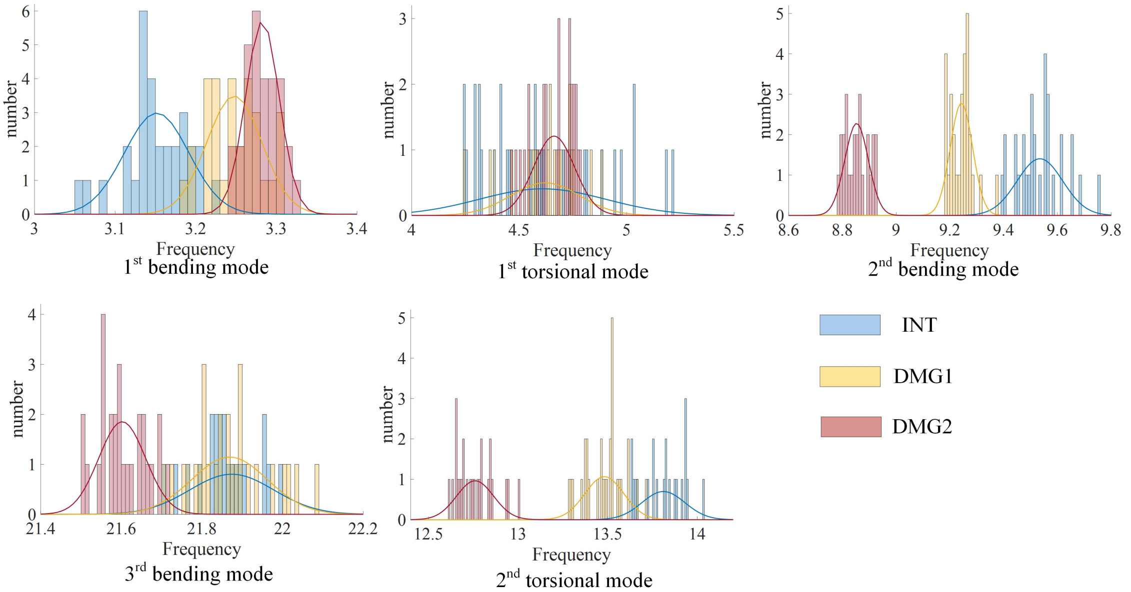

Figure 5. Histograms of the identified frequencies.

22.06Hz, 5.03Hz and 10.69Hz for the 1st, 2nd and 3rd bending modes and 1st and 2nd torsional modes, respectively.

Mode shapes obtained from the eigenvalue analysis are also shown in Fig. 4. MAC value between mode shapes from the eigenvalue analysis and those identified from experimental data were 0.96 for the 2nd torsional mode and more than 0.99 for the other modes. This means the mode shapes from the eigenvalue analysis and experiment were comparable with each other. According to the FE analysis the frequencies for all modes decreased according to damage severity. The decrease of the 1st bending frequency was much less than the frequencies of the other modes. Changes in frequency due to the damage obtained from the eigenvalue analysis showed similar tendency to those from experiment data except the 1st bending and torsional modes.

It is noteworthy that the frequency distribution of the 1st bending mode moved to higher frequency region in the order of INT, DMG1 and DMG2 in the experiment as shown in Fig. 5. One reason might be change in the boundary condition at Ab2 abutment since the longitudinal reaction at the support by deflection under deadload was increased due to the damage and led to increasing spring constant at the support, which was found from a sensitivity analysis for the change in stiffness and longitudinal spring constant at the support.

4.2 Feature extraction and damage detection

The relationship between the modal properties and the proposed damage sensitive feature is investigated in advance to the local damage detection. In the following discussions, data obtained from the intact bridge is adopted as the reference data. As mentioned in Section 2.2, the damage sensitive features are extracted according to the posterior distribution under the given reference data. The damage sensitive features can be converted to modal properties considering the relevant state space model (Goi & Kim 2018).

Fig. 6 shows six mode shapes identified from the vector regressive model reproduced by the damage sensitive features. Apparently, the extracted damage sensitive features are relevant to the bending and torsional modes listed in Fig. 4. This observation is comparable to both of the experimental modal identification and analytical results from the FE model.

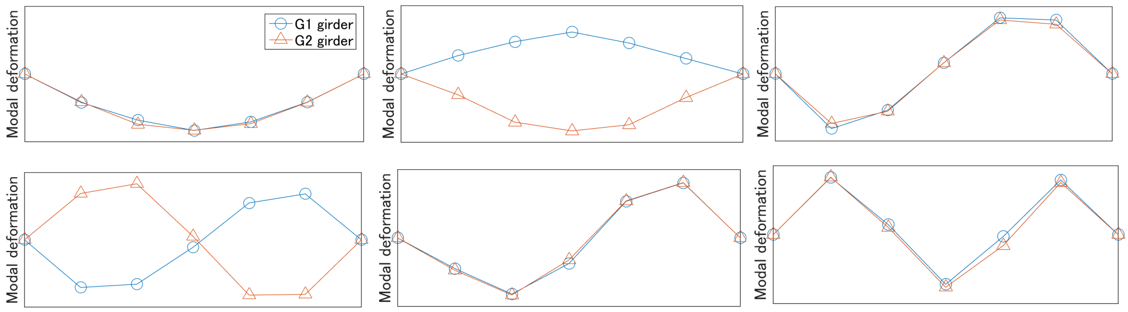

Figure 6. Mode shapes relevant to the damage sensitive features.

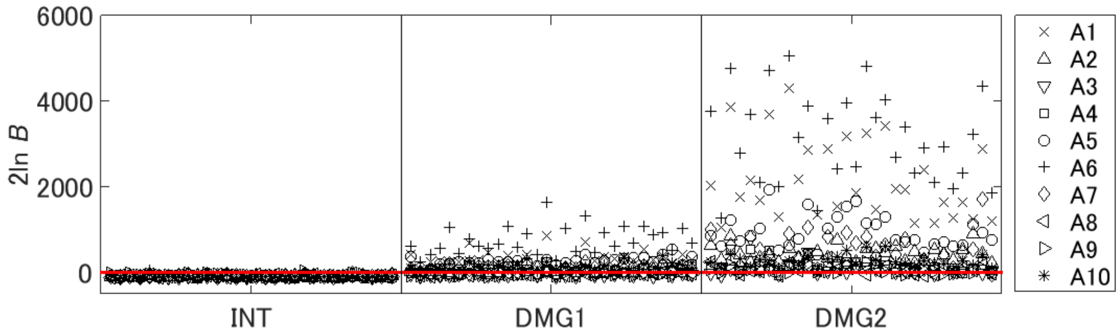

Figure 7. Bayes factors for the damage experiment.

According to the above discussions, the Bayes factor discussed hereafter presumably evaluates changes in the modal properties of the six modes observed in Fig. 4 and Fig. 6. The first 30 samples measured under the INT scenario are adopted as the reference data. The latter 30 samples are adopted as test samples for validation. The time series measured under DMG1 and DMG2 scenarios are adopted as the test samples for damage detection.

Bayes factor given in Eq. 10 enables to quantify anomaly at each of the measurement locations. Fig. 7 shows the observed Bayes factors. Here, each of the markers depicts the Bayes factor calculated for measurement location A1 to A10, for each of the vehicle loadings. The red horizontal line is the critical value such that the evidence function of the null and alternative hypotheses are equivalent, i.e., $2\ln B = 0$. When the Bayes factor exceeds the critical values, the changes in damage sensitive features are detected.

The Bayes factors promptly enable to detect anomaly caused by the damage. This observation indicates that the changes in modal properties in the six modes listed in Fig. 6 are concisely detected by the proposed Bayes factor. Furthermore, the severity of the damage is successfully quantified in the results. It is also noteworthy that the local Bayes factors at A1 and A6, which are nearest to the Ab1 abutment, are relatively higher than the others are as shown in Fig. 7. Although the precise location of the damage is not identified from those results since the Bayes factors at A6 provides relatively higher values than A1 that is nearer to the damage location, rough estimation of the damage location is still possible.

5 CONCLUSIONS

This study investigated the feasibility of damage detection of steel plate girder bridges by means of vibration-based SHM. To investigate actual behavior of the bridges, artificial damages imitating fatigue crack were introduced to an actual plate girder bridge and vehicle loading test was performed. The feasibility of the modal frequency and damage indicator using Bayesian statistics were investigated.

Modal properties identified from the experimental data and the relevant finite element model were mostly comparable. However, the frequency of the 1st bending and torsional modes resulted in an increase due to damage in the field experiment whereas those obtained from the FE model decreased. Aiming at application of FE models to convincing damage diagnosis, investigation into mechanical reason for the changes in the 1st bending and torsional modes due to damage, and how to construct reasonable FE model are remained to be solved.

The proposed feature extraction method indicated that the damage sensitive features relevant to the identified modal properties both in the experiment and FE model. The proposed hypothesis testing successfully detected changes in the modal properties due to the artificial damage. The severity of the damage is successfully quantified by the proposed damage indicator. The localized damage indicator roughly estimated the location of the damage.

ACKNOWLEDGEMENTS

This study is partly sponsored by a Japanese Society for the Promotion of Science (JSPS) Grant-in-Aid for Scientific Research (B) under project No.16H04398 and for the JSPS Fellows Project under Project No. 17 J09033. That financial support is gratefully acknowledged.

REFERENCES

Chang, K.C. & Kim, C.W. 2016. Modal-parameter identification and vibration-based damage detection of a damaged steel truss bridge. *Engineering Structures*, 122: 156-173.

Deramaeker, A., Reynders, E., De Roeck, G. & Kullaa, J. 2008. Vibration-based structural health monitoring using output-only measurements under changing environment. *Mech. Syst. Signal Process.* 22(1):34-56.

Goi, Y. & Kim, C.W. 2017. Anomaly detection of under vehicle induced vibration by means of Bayesian inference. In *Proc. of 4th Conf. on Smart Monit., Assessment and Rehabilitation of Civil Struct.* Zurich, Switzerland.

Goi, Y. & Kim, C.W. 2018. Investigation of Bayesian damage detection method for long-term bridge health monitoring. In *Proc. of 6th International Symposium on Life-Cycle Civil Engineering*, Gent, Belgium.

He, X. & De Roeck, G. 1999. Reference-based stochastic subspace identification for output-only modal analysis. *Mech. Syst. Signal Process.* 13(6):855-878.

Heylen, W., Lammens, S. & Sas, P. 1997. *Modal Analysis Theory and Testing*, Leuven: KU Leuven.

Jeffreys, H. 1946. An invariant form for the prior probability in estimation problems. In *Proc. of the Royal Society of London*. 186:453-461.

Kass, R. & Raftery, A. 1995. Bayes Factors. *Journal of the American Statistical Association*. 90(430):773-795.

McGetrick, P.J., Kim, C.W., Gonzalez, A. & O Brien, E.J. 2015. Experimental validation of a drive-by stiffness identification method for damage monitoring. *Structural Health Monitoring*, 14(4):347-331.

Nair, K.K., Kiremidjian, A.S. & Law, K.H. 2006. Time series-based damage detection and localization algorithm with application to the ASCE benchmark structure. *J. Sound Vib.* 291(1-2):349-368.

van Overschee, P. and De Moor, B. 1996. *Subspace identification for linear systems*. Norwell: Kluwer Academic Publishers.

Zhang, Q.W. 2007. Statistical damage identification for bridges using ambient vibration data. *Computers and Structures*, 85(7-8):476-485.